

电弹性耦合偏微分方程组带型裂纹问题

吴远波

吉首大学数学与统计学院, 湖南 吉首

收稿日期: 2026年3月7日; 录用日期: 2026年4月1日; 发布日期: 2026年4月13日

摘要

根据压电体中扩展的介质裂纹模型, 本文讨论了压电带型机电荷载下的Griffith裂纹问题, 在裂纹边界条件假设下, 得到一组耦合偏微分方程组。运用傅立叶变换, 将电弹性耦合偏微分方程组问题转化为求解第二类Fredholm类积分方程组。采用Lobatto-Chebyshev配置法, 得到了非线性代数方程, 并对其进行数值求解。通过数值计算分析了不同边界条件下断裂参量的变化规律并和已有实验结果进行了比较。

关键词

耦合偏微分方程组, 压电带型, 介质裂纹, 傅里叶变换

Strip Crack Problem for Electroelastic Coupled Partial Differential Equations

Yuanbo Wu

School of Mathematics and Statistics, Jishou University, Jishou Hunan

Received: March 7, 2026; accepted: April 1, 2026; published: April 13, 2026

Abstract

Based on the extended dielectric crack model in piezoelectric materials, this study examines the Griffith crack problem in piezoelectric strip structures under electromechanical loading. By assuming specific crack boundary conditions, a system of coupled partial differential equations governing the electroelastic field is formulated. Applying Fourier transforms to convert the coupled partial differential equations into a system of the second kind Fredholm integral equations. The Lobatto-Chebyshev collocation method is used to form a nonlinear system of algebraic equations, which is solved by proposing an algorithm. Numerical results are carried out to show the variations of the fracture parameters of concern on the physical properties of the dielectric inside the crack under the two boundary conditions. the formats.

Keywords

Coupled Partial Differential Equations, Piezoelectric Strip, Dielectric Crack, Fourier Transform

Copyright © 2026 by author(s) and Hans Publishers Inc.

This work is licensed under the Creative Commons Attribution International License (CC BY 4.0).

<http://creativecommons.org/licenses/by/4.0/>



Open Access

1. 引言

随着工业生产技术以及制造水平的提升,越来越多的新型材料被生产出来用以满足社会不断发展下的新要求,而压电材料就是其中之一。压电材料具有将电能转换为机械能的良好物理特性反之亦然,这使得多场耦合效应下的压电体被广泛应用在发电机、传感器以及制动器等智能器件上。然而压电陶瓷本身具有脆性,在实际生产和使用过程中不可避免的出现裂纹缺陷。因此为了解智能器件的稳定性,有必要研究压电固体在不同荷载下的断裂行为[1][2]。在理论研究中发现,压电固体中裂纹的扩展依赖于许多因素,如裂纹尖端非弹性变形[3]、裂纹尖端区域转换[4]和裂纹内部的介电效应[5]。另外,文献[6]考虑含圆币型介质裂纹压电体在机电荷载作用下,通过引进势函数来分析其断裂行为,并导出了裂纹尖端的应力场和电位移场。文献[7][8]考虑到开口裂纹内介质的存在和裂纹表面电场可导,分析了电场对压电层中圆币型介质裂纹扩张的影响。文献[9][10]分别假设在裂纹内电场式绝缘和可导的情形下,求解出压电介质的应力强度因子和能量释放率,并分析压电体的裂纹位置参数和外加荷载对它们的影响。文献[11][12]基于有限厚度的压电层裂纹问题,同样讨论了电场对压电介质的应力强度因子和能量释放率的影响。而文献[13]考虑横观各向同性压电材料,通过将外加电荷载视为瞬态冲击过程,研究其纯电荷载作用下的电不透 III 型裂纹的动态响应。

基于以上研究,本文利用扩展介质裂纹模型,重点分析含带型裂纹的有限厚度压电体在机电荷载作用下的断裂行为。通过数值模拟,讨论在两类不同边界条件下,裂纹内介质的介电常数对电位移和电位强度因子的影响。结果表明用自由法向应力边界条件近似模拟实际情况是可行的。

2. 研究对象

考虑横观各向同性压电带型中嵌入一个 Griffith 裂纹的情形,如图 1 所示。建立直角坐标系,裂纹位于沿 x 轴 $-a < x < a$ 处, Z 轴垂直于裂纹面,横观各向同性压电体厚度为 $h_1 + h_{II} = 2h$,其中 h_1 (或者 h_{II}) 代表裂纹面到压电体上(或者下)表面的距离。假设裂纹内部充满介电常数为 ϵ_c 的介质,机械荷载 σ_0 作用

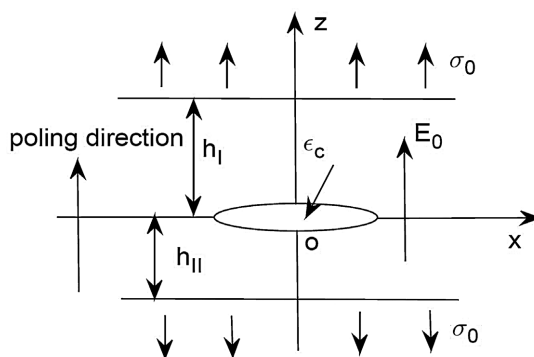


Figure 1. A dielectric crack in a piezoelectric strip
图 1. 压电带型中的介质裂纹

于压电体表面，另外 E_0 是电场荷载。

在平面内的机电荷载作用下，利用线性压电理论，有如下本构方程[1]：

$$\sigma_{xx}^j = c_{11} \frac{\partial u_x^j}{\partial x} + c_{13} \frac{\partial u_z^j}{\partial z} + e_{31} \frac{\partial \phi^j}{\partial z}, \quad (1)$$

$$\sigma_{zz}^j = c_{13} \frac{\partial u_x^j}{\partial x} + c_{33} \frac{\partial u_z^j}{\partial z} + e_{33} \frac{\partial \phi^j}{\partial z}, \quad (2)$$

$$\sigma_{xz}^j = c_{44} \left(\frac{\partial u_x^j}{\partial z} + \frac{\partial u_z^j}{\partial x} \right) + e_{15} \frac{\partial \phi^j}{\partial x}, \quad (3)$$

$$D_x^j = e_{15} \left(\frac{\partial u_x^j}{\partial z} + \frac{\partial u_z^j}{\partial x} \right) - \varepsilon_{11} \frac{\partial \phi^j}{\partial x}, \quad (4)$$

$$D_z^j = e_{31} \frac{\partial u_x^j}{\partial x} + e_{33} \frac{\partial u_z^j}{\partial z} - \varepsilon_{33} \frac{\partial \phi^j}{\partial z}, \quad (5)$$

其中 $j = \text{I}$ 或者 II 。 σ_x^j 、 u_x^j 和 D_x^j 分别代表应力，弹性位移和电位移。 ϕ^j 代表电势， c_x 、 e_x 和 ε_x 分别表示弹性刚度，压电常数和介电常数。

在忽略体积力和自由电荷等情况下，运用平衡微分方程，可得到下面的耦合偏微分微分方程组：

$$c_{11} \frac{\partial^2 u_x^j}{\partial x^2} + c_{44} \frac{\partial^2 u_z^j}{\partial z^2} + (c_{13} + c_{44}) \frac{\partial^2 u_z^j}{\partial x \partial z} + (e_{31} + e_{15}) \frac{\partial^2 \phi^j}{\partial x \partial z} = 0, \quad (6)$$

$$c_{44} \frac{\partial^2 u_x^j}{\partial x^2} + c_{33} \frac{\partial^2 u_z^j}{\partial z^2} + (c_{13} + c_{44}) \frac{\partial^2 u_x^j}{\partial x \partial z} + e_{15} \frac{\partial^2 \phi^j}{\partial x^2} + e_{33} \frac{\partial^2 \phi^j}{\partial z^2} = 0, \quad (7)$$

$$e_{15} \frac{\partial^2 u_z^j}{\partial x^2} + e_{33} \frac{\partial^2 u_z^j}{\partial z^2} + (e_{31} + e_{15}) \frac{\partial^2 u_x^j}{\partial x \partial z} - \varepsilon_{11} \frac{\partial^2 \phi^j}{\partial x^2} - \varepsilon_{33} \frac{\partial^2 \phi^j}{\partial z^2} = 0, \quad (8)$$

为刻画裂纹中充满介质，其裂纹面上的边界条件为：

$$\sigma_{xz}^{\text{I}}(x, 0) = \sigma_{xz}^{\text{II}}(x, 0) = 0, \quad -a < x < a, \quad (9)$$

$$\sigma_{zz}^{\text{I}}(x, 0) = \sigma_{zz}^{\text{II}}(x, 0) = 0, \quad -a < x < a, \quad (10)$$

$$D_z^{\text{I}}(x, 0) = D_z^{\text{II}}(x, 0) = D_c, \quad -a < x < a, \quad (11)$$

其中

$$D_c = -\varepsilon_c \frac{\phi^{\text{I}}(x, 0) - \phi^{\text{II}}(x, 0)}{u_z^{\text{I}}(x, 0) - u_z^{\text{II}}(x, 0)} + \omega_c D_0, \quad (12)$$

ω_c 是一个调整参数， D_0 代表施加的电位移， $\varepsilon_c = \varepsilon_r \varepsilon_0$ ($\varepsilon_0 = 8.85 \times 10^{-12} \text{ F/m}$) 是介电常数。另外在 $|x| > a$ 的边界条件为：

$$u_x^{\text{I}}(x, 0) = u_x^{\text{II}}(x, 0), \quad u_z^{\text{I}}(x, 0) = u_z^{\text{II}}(x, 0), \quad (13)$$

$$\phi^{\text{I}}(x, 0) = \phi^{\text{II}}(x, 0), \quad D_z^{\text{I}}(x, 0) = D_z^{\text{II}}(x, 0), \quad (14)$$

$$\sigma_{xz}^{\text{I}}(x, 0) = \sigma_{xz}^{\text{II}}(x, 0), \quad \sigma_{zz}^{\text{I}}(x, 0) = \sigma_{zz}^{\text{II}}(x, 0), \quad (15)$$

而在压电带型表面的边界条件为：

$$\sigma_{zz}^{\text{I}}(x, h_1) = \sigma_{zz}^{\text{II}}(x, -h_{11}) = \sigma_0, \quad (16)$$

$$E_z^I(x, h_1) = E_z^{II}(x, -h_{II}) = E_0, \tag{17}$$

考虑压电带型表面有自由剪应力时, 有

$$\sigma_{xz}^I(x, h_1) = \sigma_{xz}^{II}(x, -h_{II}) = 0, \tag{18}$$

而根据文献[7], 假定压电层表面沿 x 方向的法向应力为零, 可得

$$\sigma_{xx}^I(x, h_1) = \sigma_{xx}^{II}(x, -h_{II}) = 0, \tag{19}$$

根据文献[4]的研究表明自由剪应力条件(23)是可行的, 不需要自由法向应力条件(24)。然而, 文献[13]表明, 压电带型表面的自由法向应力条件与实际情况很接近。在本文中, 分别以边界条件(23)和(24)来计算压电带型裂纹尖端的电弹性场, 并且与文献[9]实验结果进行比较。

3. 求解过程

3.1. 电弹性场的求解

这里我们主要求解的是由机电荷载引起的电弹性场。利用傅里叶变换, 微分方程(6)~(8)的解可以表示成如下形式

$$u_x^j(x, z) = \sum_{i=1}^3 \int_0^\infty \left[A_i^j(\xi) \cosh(-\delta^j \alpha_i z \xi) + B_i^j(\xi) \sinh(-\delta^j \alpha_i z \xi) \right] \sin(\xi x) d\xi + C_0 x, \tag{20}$$

$$u_z^j(x, z) = \sum_{i=1}^3 \int_0^\infty \eta_{3i} \alpha_i \delta^j \left[A_i^j(\xi) \sinh(-\delta^j \alpha_i z \xi) + B_i^j(\xi) \cosh(-\delta^j \alpha_i z \xi) \right] \cos(\xi x) d\xi + C_1 z, \tag{21}$$

$$\phi^{Gj}(x, z) = \sum_{i=1}^3 \int_0^\infty \eta_{4i} \alpha_i \delta^j \left[A_i^j(\xi) \sinh(-\delta^j \alpha_i z \xi) + B_i^j(\xi) \cosh(-\delta^j \alpha_i z \xi) \right] \cos(\xi x) d\xi + C_2 z, \tag{22}$$

其中 $A_i^j(\xi)$ 和 $B_i^j(\xi)$ 是待求解的未知函数, $\delta^I = 1$ 以及 $\delta^{II} = 1$ 。常数 α_i , η_{3i} 和 η_{4i} 将在附录 A 中给出。另外 C_0 , C_1 和 C_2 可由边界条件确定。

将上述微分方程的解(20)~(22)带入到本构方程(1)~(5), 应力和电位移的表达式可以写成

$$\begin{bmatrix} \sigma_{xx}^j(x, z) \\ \sigma_{zz}^j(x, z) \\ D_z^j(x, z) \end{bmatrix} = \sum_{i=1}^3 \begin{bmatrix} \gamma_{0i} \\ \gamma_{1i} \\ \gamma_{2i} \end{bmatrix} \int_0^\infty \xi \left[A_i^j(\xi) \cosh(-\delta^j \alpha_i z \xi) + B_i^j(\xi) \sinh(-\delta^j \alpha_i z \xi) \right] \cos(\xi x) d\xi + \begin{bmatrix} c_{11} & c_{13} & e_{31} \\ c_{13} & c_{33} & e_{33} \\ e_{31} & e_{33} & -\epsilon_{33} \end{bmatrix} \begin{bmatrix} C_0 \\ C_1 \\ C_2 \end{bmatrix}, \tag{23}$$

$$\begin{bmatrix} \sigma_{xz}^j(x, z) \\ D_x^j(x, z) \end{bmatrix} = \sum_{i=1}^3 \begin{bmatrix} \gamma_{3i} \\ \gamma_{4i} \end{bmatrix} \int_0^\infty \delta^j \xi \left[A_i^j(\xi) \sinh(-\delta^j \alpha_i z \xi) + B_i^j(\xi) \cosh(-\delta^j \alpha_i z \xi) \right] \sin(\xi x) d\xi, \tag{24}$$

其中常数 γ_{ij} 在附录 A 中给出。

为确定未知函数 $A_i^j(\xi)$ 和 $B_i^j(\xi)$, 引进辅助函数 $\Phi_i(x)$ ($i = 1, 2, 3$) 如下:

$$\begin{bmatrix} \Phi_1(x) \\ \Phi_2(x) \\ \Phi_3(x) \end{bmatrix} = \frac{\partial}{\partial x} \begin{bmatrix} u_x^I(x, 0) - u_x^{II}(x, 0) \\ u_z^I(x, 0) - u_z^{II}(x, 0) \\ \phi^I(x, 0) - \phi^{II}(x, 0) \end{bmatrix}, \tag{25}$$

结合边界条件(13)~(14)并且运用傅里叶逆变换可得

$$\sum_{i=1}^3 [A_i^I(\xi) - A_i^{II}(\xi)] = \frac{2}{\pi\xi} \int_0^a \Phi_1(s) \cos(\xi s) ds, \tag{26}$$

$$\sum_{i=1}^3 \eta_{3i} \alpha_i [B_i^I(\xi) + B_i^{II}(\xi)] = -\frac{2}{\pi\xi} \int_0^a \Phi_2(s) \sin(\xi s) ds, \tag{27}$$

$$\sum_{i=1}^3 \eta_{4i} \alpha_i [B_i^I(\xi) + B_i^{II}(\xi)] = -\frac{2}{\pi\xi} \int_0^a \Phi_3(s) \sin(\xi s) ds, \tag{28}$$

另外不难得出电场 $E_z^j(x, z)$ 的表达式如下:

$$E_z^j(x, z) = \sum_{i=1}^3 \int_0^\infty \eta_{4i} \alpha_i^2 \xi [A_i^j(\xi) \cosh(-\delta^j \alpha_i z \xi) + B_i^j(\xi) \sinh(-\delta^j \alpha_i z \xi)] \cos(\xi x) d\xi - C_2$$

利用条件(17)有 $C_2 = -E_0$ 以及

$$\sum_{i=1}^3 \eta_{4i} \alpha_i^2 [A_i^j(\xi) \cosh(-\alpha_i h_j \xi) + B_i^j(\xi) \sinh(-\alpha_i h_j \xi)] = 0, \tag{29}$$

显然条件利用条件(16)和(18)不能求出 C_0 和 C_1 , 此时 C_0 和 C_1 取与由条件(16)和(19)求出的值相同, 即

$$C_0 = \frac{-c_{11}\sigma_0 + (c_{33}e_{31} - c_{13}e_{33})E_0}{c_{11}c_{33} - c_{13}^2}, \quad C_1 = \frac{c_{11}\sigma_0 + (c_{11}e_{33} - c_{13}e_{31})E_0}{c_{11}c_{33} - c_{13}^2},$$

并且有

$$D_0 = \frac{c_{11}e_{33} - c_{13}e_{31}}{c_{11}c_{33} - c_{13}^2} \sigma_0 + \left(\frac{c_{33}e_{31}^2 + c_{11}e_{33}^2 - 2c_{13}e_{33}e_{31}}{c_{11}c_{33} - c_{13}^2} + \epsilon_{33} \right) E_0,$$

根据条件(16)有

$$\sum_{i=1}^3 \gamma_{1i} [A_i^j(\xi) \cosh(-\alpha_i h_j \xi) + B_i^j(\xi) \sinh(-\alpha_i h_j \xi)] = 0, \tag{30}$$

为方便进行比较, 分两类情形分析, 根据式(18)和(23)有

$$\text{情形 I: } \sum_{i=1}^3 \gamma_{3i} [A_i^j(\xi) \sinh(-\alpha_i h_j \xi) + B_i^j(\xi) \cosh(-\alpha_i h_j \xi)] = 0, \tag{31}$$

由式(19)和(22)可得

$$\text{情形 II: } \sum_{i=1}^3 \gamma_{0i} [A_i^j(\xi) \cosh(-\alpha_i h_j \xi) + B_i^j(\xi) \sinh(-\alpha_i h_j \xi)] = 0, \tag{32}$$

另外根据边界条件(9)~(11)以及(13)~(15)可以得到

$$\sum_{i=1}^3 \gamma_{1i} [A_i^I(\xi) - A_i^{II}(\xi)] = 0, \tag{33}$$

$$\sum_{i=1}^3 \gamma_{2i} [A_i^I(\xi) - A_i^{II}(\xi)] = 0, \tag{34}$$

$$\sum_{i=1}^3 \gamma_{3i} [A_i^I(\xi) - A_i^{II}(\xi)] = 0, \tag{35}$$

综合式(26)~(28)和(30)~(35), 未知函数 $A_i^j(\xi)$ 和 $B_i^j(\xi)$ 可以表示为

$$\Pi = [b_{ij}(\xi)]_{12 \times 12} \begin{bmatrix} \frac{2}{\pi\xi} \int_0^a \Phi_1(s) \cos(\xi s) ds \\ -\frac{2}{\pi\xi} \int_0^a \Phi_2(s) \sin(\xi s) ds \\ -\frac{2}{\pi\xi} \int_0^a \Phi_3(s) \sin(\xi s) ds \\ 0 \\ \vdots \\ 0 \end{bmatrix}, \tag{36}$$

其中 $\Pi = [A_1^I(\xi) \ A_2^I(\xi) \ \dots \ A_3^II(\xi) \ B_1^I(\xi) \ B_2^I(\xi) \ \dots \ B_3^II(\xi)]^T$ 。为节省空间，系数矩阵 $[b_{ij}(\xi)]_{12 \times 12}$ 省略。

另外利用式(13)~(15)结合(36)有

$$\begin{aligned} & \frac{2}{\pi} \sum_{i=1}^3 \gamma_{1i} \left[\int_0^a \Phi_1(s) ds \int_0^\infty b_{i1}(\xi) \cos(\xi s) \cos(\xi x) d\xi \right. \\ & \left. - \sum_{j=2}^3 \int_0^a \Phi_j(s) ds \int_0^\infty b_{ij}(\xi) \sin(\xi s) \cos(\xi x) d\xi \right] = -\sigma_0, \end{aligned} \tag{37}$$

$$\begin{aligned} & \frac{2}{\pi} \sum_{i=1}^3 \gamma_{2i} \left[\int_0^a \Phi_1(s) ds \int_0^\infty b_{i1}(\xi) \cos(\xi s) \cos(\xi x) d\xi \right. \\ & \left. - \sum_{j=2}^3 \int_0^a \Phi_j(s) ds \int_0^\infty b_{ij}(\xi) \sin(\xi s) \cos(\xi x) d\xi \right] = -(D_0 - D_c), \end{aligned} \tag{38}$$

$$\begin{aligned} & \frac{2}{\pi} \sum_{i=1}^3 \gamma_{3i} \left[\int_0^a \Phi_1(s) ds \int_0^\infty b_{(i+6)1}(\xi) \cos(\xi s) \sin(\xi x) d\xi \right. \\ & \left. - \sum_{j=2}^3 \int_0^a \Phi_j(s) ds \int_0^\infty b_{(i+6)j}(\xi) \sin(\xi s) \cos(\xi x) d\xi \right] = 0. \end{aligned} \tag{39}$$

令 $\lim_{\xi \rightarrow \infty} \sum_{i=1}^3 \gamma_{ki} b_{ij}(\xi) = x_{kj} \ (k=1,2; j=2,3)$ ， $\lim_{\xi \rightarrow \infty} \sum_{i=1}^3 \gamma_{ki} b_{(i+6)j}(\xi) = x_{kj} \ (k=3, j=1)$ ，以及引进变量变换

$$x = a\bar{x}, \quad s = a\bar{s}, \quad \Phi_i(s) = \frac{\bar{\Phi}_i(\bar{s})}{\sqrt{1-\bar{s}^2}}, \quad i=1,2,3,$$

并且利用已知结果：

$$2 \int_0^\infty \sin(\xi s) \cos(\xi x) d\xi = \frac{1}{s-x} + \frac{1}{s+x},$$

则式(37)~(39)重新改写为

$$\begin{aligned} & \frac{1}{\pi} \int_{-1}^1 \frac{\bar{\Phi}_1(\bar{s})}{\sqrt{1-\bar{s}^2}} \kappa_{11}(\bar{s}, \bar{x}) d\bar{s} - \frac{1}{\pi} \int_{-1}^1 \left[\frac{x_{12}}{\bar{s}-\bar{x}} + \kappa_{12}(\bar{s}, \bar{x}) \right] \frac{\bar{\Phi}_2(\bar{s})}{\sqrt{1-\bar{s}^2}} d\bar{s} \\ & - \frac{1}{\pi} \int_{-1}^1 \left[\frac{x_{13}}{\bar{s}-\bar{x}} + \kappa_{13}(\bar{s}, \bar{x}) \right] \frac{\bar{\Phi}_3(\bar{s})}{\sqrt{1-\bar{s}^2}} d\bar{s} = -\sigma_0, \end{aligned} \tag{40}$$

$$\begin{aligned} & \frac{1}{\pi} \int_{-1}^1 \frac{\bar{\Phi}_1(\bar{s})}{\sqrt{1-\bar{s}^2}} \kappa_{21}(\bar{s}, \bar{x}) d\bar{s} - \frac{1}{\pi} \int_{-1}^1 \left[\frac{x_{22}}{\bar{s}-\bar{x}} + \kappa_{22}(\bar{s}, \bar{x}) \right] \frac{\bar{\Phi}_2(\bar{s})}{\sqrt{1-\bar{s}^2}} d\bar{s} \\ & - \frac{1}{\pi} \int_{-1}^1 \left[\frac{x_{23}}{\bar{s}-\bar{x}} + \kappa_{23}(\bar{s}, \bar{x}) \right] \frac{\bar{\Phi}_3(\bar{s})}{\sqrt{1-\bar{s}^2}} d\bar{s} = -(D_0 - D_c), \end{aligned} \tag{41}$$

$$\begin{aligned} & \frac{1}{\pi} \int_{-1}^1 \left[\frac{x_{31}}{\bar{s} - \bar{x}} + \kappa_{31}(\bar{s}, \bar{x}) \right] \frac{\bar{\Phi}_1(\bar{s})}{\sqrt{1 - \bar{s}^2}} d\bar{s} - \frac{1}{\pi} \int_{-1}^1 \frac{\bar{\Phi}_2(\bar{s})}{\sqrt{1 - \bar{s}^2}} \kappa_{32}(\bar{s}, \bar{x}) d\bar{s} \\ & - \frac{1}{\pi} \int_{-1}^1 \frac{\bar{\Phi}_3(\bar{s})}{\sqrt{1 - \bar{s}^2}} \kappa_{33}(\bar{s}, \bar{x}) d\bar{s} = 0. \end{aligned} \tag{42}$$

其中函数 $\kappa_{ij}(\bar{s}, \bar{x}) (i, j = 1, 2, 3)$ 在附录 A 中给出。此外考虑到还要满足约束条件

$$\int_{-a}^a \Phi_i(s) ds = \int_{-1}^1 \frac{\bar{\Phi}_i(\bar{s})}{\sqrt{1 - \bar{s}^2}} d\bar{s} = 0, \quad (i = 1, 2, 3). \tag{43}$$

众所周知奇异积分方程有很多种数值解法，这里我们运用 Lobatto-Chebyshev 配置法，可得到以下代数方程组：

$$\begin{aligned} & \frac{1}{n} \sum_{l=0}^n \lambda_l \kappa_{11}(\bar{s}_l, \bar{x}_m) \bar{\Phi}_1(\bar{s}_l) - \frac{1}{n} \sum_{l=0}^n \lambda_l \left[\frac{x_{12}}{\bar{s}_l - \bar{x}_m} + \kappa_{12}(\bar{s}_l, \bar{x}_m) \right] \bar{\Phi}_2(\bar{s}_l) \\ & - \frac{1}{n} \sum_{l=0}^n \lambda_l \left[\frac{x_{13}}{\bar{s}_l - \bar{x}_m} + \kappa_{13}(\bar{s}_l, \bar{x}_m) \right] \bar{\Phi}_3(\bar{s}_l) = -\sigma_0, \end{aligned} \tag{44}$$

$$\begin{aligned} & \frac{1}{n} \sum_{l=0}^n \lambda_l \kappa_{21}(\bar{s}_l, \bar{x}_m) \bar{\Phi}_1(\bar{s}_l) - \frac{1}{n} \sum_{l=0}^n \lambda_l \left[\frac{x_{22}}{\bar{s}_l - \bar{x}_m} + \kappa_{22}(\bar{s}_l, \bar{x}_m) \right] \bar{\Phi}_2(\bar{s}_l) \\ & - \frac{1}{n} \sum_{l=0}^n \lambda_l \left[\frac{x_{23}}{\bar{s}_l - \bar{x}_m} + \kappa_{23}(\bar{s}_l, \bar{x}_m) \right] \bar{\Phi}_3(\bar{s}_l) = -(D_0 - D_c), \end{aligned} \tag{45}$$

$$\begin{aligned} & \frac{1}{n} \sum_{l=0}^n \lambda_l \left[\frac{x_{31}}{\bar{x}_m - \bar{s}_l} + \kappa_{31}(\bar{s}_l, \bar{x}_m) \right] \bar{\Phi}_1(\bar{s}_l) - \frac{1}{n} \sum_{l=0}^n \lambda_l \kappa_{32}(\bar{s}_l, \bar{x}_m) \bar{\Phi}_2(\bar{s}_l) \\ & - \frac{1}{n} \sum_{l=0}^n \lambda_l \kappa_{33}(\bar{s}_l, \bar{x}_m) \bar{\Phi}_3(\bar{s}_l) = 0, \end{aligned} \tag{46}$$

$$\sum_{l=0}^n \lambda_l \bar{\Phi}_i(\bar{s}_l) = 0, \tag{47}$$

其中

$$\bar{x} = \cos[(2m-1)\pi/(2n)], \quad m = 1, 2, \dots, n,$$

$$\bar{s}_l = \cos(l\pi/n), \quad l = 0, 1, \dots, n,$$

$$\lambda_0 = \lambda_n = 1/2, \quad \lambda_1 = \dots = \lambda_{n-1} = 1.$$

显然要求解代数方程组(44)~(47)，应该先确定未知量 D_c 。一旦 D_c 已知，机电荷载作用下的电弹性场也就确定了。

3.2. 电场强度因子

在确定电场强度因子前，首先求出 D_c ，根据式(25)有

$$u_z^I(x, 0) - u_z^{II}(x, 0) = -a \int_{\bar{x}}^1 \frac{\bar{\Phi}_2(\bar{s})}{\sqrt{1 - \bar{s}^2}} d\bar{s}, \quad |\bar{x}| < 1, \tag{48}$$

$$\phi^I(x, 0) - \phi^{II}(x, 0) = -a \int_{\bar{x}}^1 \frac{\bar{\Phi}_3(\bar{s})}{\sqrt{1 - \bar{s}^2}} d\bar{s}, \quad |\bar{x}| < 1. \tag{49}$$

另外再结合式(12)可得

$$(D_c - \omega_c D_0) \sum_{l=0}^{n/2} \lambda_l \bar{\Phi}_2(\bar{s}_l) + \varepsilon_c \sum_{l=0}^{n/2} \lambda_l \bar{\Phi}_3(\bar{s}_l) = 0, \tag{50}$$

显然式(44)~(47)和(50)组成一个非线性代数方程组。为了方便，将式(44)~(47)改写为

$$C_{(3n+3) \times (3n+3)} \cdot Y = S,$$

或者

$$Y = C_{(3n+3) \times (3n+3)}^{-1} \cdot S, \tag{51}$$

其中 $C_{(3n+3) \times (3n+3)}$ 是系数矩阵，向量 Y 和 S 表达式如下：

$$Y = [\bar{\Phi}_1(\bar{s}_0), \dots, \bar{\Phi}_1(\bar{s}_n), \bar{\Phi}_2(\bar{s}_0), \dots, \bar{\Phi}_2(\bar{s}_n), \bar{\Phi}_3(\bar{s}_0), \dots, \bar{\Phi}_3(\bar{s}_n)]^T,$$

$$S = \left[\underbrace{-\sigma_0, \dots, -\sigma_0}_n, \underbrace{-D_0 + D^c, \dots, -D_0 + D^c}_n, \underbrace{0, \dots, 0}_{n+3} \right]^T,$$

将式(51)代入到(50)可得

$$D \cdot C_{(3n+3) \times (3n+3)}^{-1} \cdot S = 0, \tag{52}$$

其中

$$D = \left[\underbrace{0, \dots, 0}_{n+1}, \underbrace{(D_c - \omega_c D_0) \lambda_0, \dots, (D_c - \omega_c D_0) \lambda_{n/2}}_{1+n/2}, \underbrace{0, \dots, 0}_{n/2}, \underbrace{\varepsilon_c \lambda_0, \dots, \varepsilon_c \lambda_{n/2}}_{1+n/2}, \underbrace{0, \dots, 0}_{n/2} \right].$$

由此可知，一旦式(52)被求解出来，未知量 D_c 也就确定下来了，再将已知的 D_c 代入到式(51)，这样向量 Y 也确定了。

根据前面的分析，不难得到下面式子

$$\sigma_{xz}^I(x, 0) = -\frac{x_{12}}{\pi} \int_{-1}^1 \frac{\bar{\Phi}_2(\bar{s})}{(\bar{s} - \bar{x})\sqrt{1 - \bar{s}^2}} d\bar{s} - \frac{x_{13}}{\pi} \int_{-1}^1 \frac{\bar{\Phi}_3(\bar{s})}{(\bar{s} - \bar{x})\sqrt{1 - \bar{s}^2}} d\bar{s} + O(1),$$

$$D_z^I(x, 0) = -\frac{x_{22}}{\pi} \int_{-1}^1 \frac{\bar{\Phi}_2(\bar{s})}{(\bar{s} - \bar{x})\sqrt{1 - \bar{s}^2}} d\bar{s} - \frac{x_{23}}{\pi} \int_{-1}^1 \frac{\bar{\Phi}_3(\bar{s})}{(\bar{s} - \bar{x})\sqrt{1 - \bar{s}^2}} d\bar{s} + O(1),$$

$$\sigma_{xz}^I(x, 0) = \frac{x_{31}}{\pi} \int_{-1}^1 \frac{\bar{\Phi}_1(\bar{s})}{(\bar{s} - \bar{x})\sqrt{1 - \bar{s}^2}} d\bar{s} + O(1).$$

这样我们就可以得到应力强度因子和电位移强度因子如

$$K_I = \lim_{x \rightarrow a^+} \sqrt{2\pi(x-a)} \sigma_{zz}^I(x, 0) = [x_{12} \bar{\Phi}_2(1) + x_{13} \bar{\Phi}_3(1)] \sqrt{\pi a},$$

$$K_D = \lim_{x \rightarrow a^+} \sqrt{2\pi(x-a)} D_z^I(x, 0) = [x_{22} \bar{\Phi}_2(1) + x_{23} \bar{\Phi}_3(1)] \sqrt{\pi a},$$

$$K_{II} = \lim_{x \rightarrow a^+} \sqrt{2\pi(x-a)} \sigma_{xz}^I(x, 0) = x_{31} \bar{\Phi}_1(1) \sqrt{\pi a}.$$

另一方面，根据式(25)可得裂纹张开位移强度因子以及电位强度因子

$$K_{COD} = \lim_{x \rightarrow a^-} \sqrt{\frac{\pi}{2(a-x)}} \frac{u_z^I(x,0) - u_z^{II}(x,0)}{2} = -\frac{\bar{\Phi}_2(1)}{2} \sqrt{\pi a}, \quad (53)$$

$$K_\phi = \lim_{x \rightarrow a^-} \sqrt{\frac{\pi}{2(a-x)}} \frac{\phi^I(x,0) - \phi^{II}(x,0)}{2} = -\frac{\bar{\Phi}_3(1)}{2} \sqrt{\pi a}. \quad (54)$$

4. 数值实例分析

现在我们通过数值实例来分析压电带型在机电荷载作用下，两种情形边界条件的电弹性场，选取的压电材料参数数据如下表 1 所示：

Table 1. Material constants of a piezoelectric solid
表 1. 压电固体的材料参数

c_{11}	c_{13}	c_{33}	c_{44}	e_{31}	e_{33}	e_{15}	ϵ_{11}	ϵ_{33}
106.08	49.32	79.67	23.26	-17.6708	19.9165	20.8140	234.1	159.5

单位：弹性常数(GPa)；压电常数(C/m²)；介电常数($\times 10^{-10}$ C/V m)。

利用上面的数据，通过数值计算有

$$x_{12} = -1.7315 \times 10^{10}, \quad x_{13} = x_{22} = -0.80793,$$

$$x_{23} = 1.4794 \times 10^{-8}, \quad x_{31} = -2.5009 \times 10^{10}.$$

首先，讨论在两种情形边界条件下，裂纹内的介电常数对电位移的影响，如图 2 所示。从图中我们可以知道，随着 ϵ_r 地增加，电位移 D_c 也增加，这与文献[7]中的结论是一致的。另一方面，通过对情形 I 和情形 II 的比较，发现两种边界条件下的结果存在明显差异。为进一步分析这种差异，我们研究裂纹上的电势差并与文献[11]中的结论相比较。图 3 展示了在情形 I 和情形 II 的边界条件下，归一化后的电位强度因子随介电常数的变化趋势。由图可知，对任意 ϵ_r ，归一化后的电位强度因子都是小于 0 的，这个实验现象与文献[2]相符合。另外，当 ϵ_r 不断增大时， $K_\phi/E_0\sqrt{\pi a}$ 的绝对值减小，这意味着随着裂纹内部渗透性的增加，裂纹上下表面电势差在减小。

根据文献[9]的实验结果可知，当 $\epsilon_r = 40$ 时，弹性位移差和电势差如下

$$\Delta u_z [\text{nm}] = 32.30\sqrt{r[\mu\text{m}]}, \quad \Delta\phi [\text{V}] = -0.37\sqrt{r[\mu\text{m}]}, \quad (55)$$

其中 r 表示到裂纹尖端的距离。根据式(53)和(54)，裂纹尖端处弹性位移差和电势差可近似表示为

$$u_z^I(x,0) - u_z^{II}(x,0) \approx -\sqrt{2a}\bar{\Phi}_2(1)\sqrt{r}, \quad (56)$$

$$\phi^I(x,0) - \phi^{II}(x,0) \approx -\sqrt{2a}\bar{\Phi}_3(1)\sqrt{r}, \quad (57)$$

其中有 $r \ll a$ 成立。类似文献[7]中的方法，取 $\epsilon_r = 40$ 时，根据(55)~(57)当 $\bar{\Phi}_2(1) = -0.002283955$ ，则情形 I 对应有 $\sigma_0 = 28.1$ MPa，情形 II 对应有 $\sigma_0 = 32.5$ MPa。

而电势差通过计算有：

$$\text{情形 I: } \phi^I(x,0) - \phi^{II}(x,0) = -0.6849\sqrt{r[\mu\text{m}]},$$

$$\text{情形 II: } \phi^I(x,0) - \phi^{II}(x,0) = -0.3449\sqrt{r[\mu\text{m}]}.$$

根据上面的结果可知，由情形 I 得出数值结果与文献[14]中的结论有很大的偏差，而由情形 II 得出的

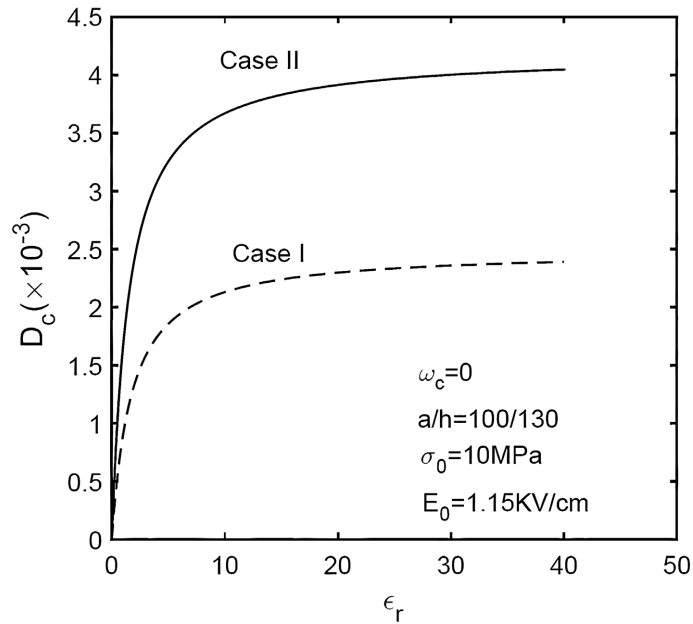


Figure 2. The variations of D_c versus ϵ_r for $E_0=1.15$ KV/cm, $\sigma_0=10$ MPa, $a/h=100/130$ and $\omega_c=0$ under Case I Case II, respectively

图 2. 电位移 D_c 随 ϵ_r 在情形 I 和情形 II 以及 $E_0=1.15$ KV/cm, $\sigma_0=10$ MPa, $a/h=100/130$ 和 $\omega_c=0$ 的变化趋势

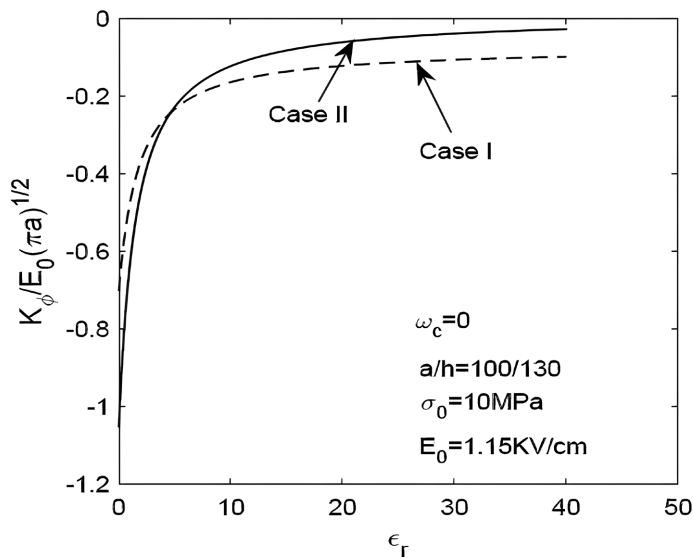


Figure 3. The variations of $K_\phi/E_0\sqrt{\pi a}$ versus ϵ_r for $E_0=1.15$ KV/cm, $\sigma_0=10$ MPa, $a/h=100/130$ and $\omega_c=0$ under Case I Case II, respectively

图 3. $K_\phi/E_0\sqrt{\pi a}$ 随 ϵ_r 在情形 I 和情形 II 以及 $E_0=1.15$ KV/cm, $\sigma_0=10$ MPa, $a/h=100/130$ 和 $\omega_c=0$ 的变化趋势

结果与文献[14]相符合。上述实验结果表明，在压电带型表面自由法向应力条件下，可以近似模拟实际情况。

在提出的扩展介质裂纹模型中，主要是引进了调节参数 ω_c ，可以用来调整实验结果与理论观测结果之间的差异。如图 4 中展示了当 ω_c 取 -0.1, 0, 0.1 时， $K_\phi/E_0\sqrt{\pi a}$ 随 ϵ_r 以及 ω_c 的变化情况。由图可知，固定 ϵ_r 的值， ω_c 的增大会导致 $K_\phi/E_0\sqrt{\pi a}$ 增大，这就起到了一个调整作用。

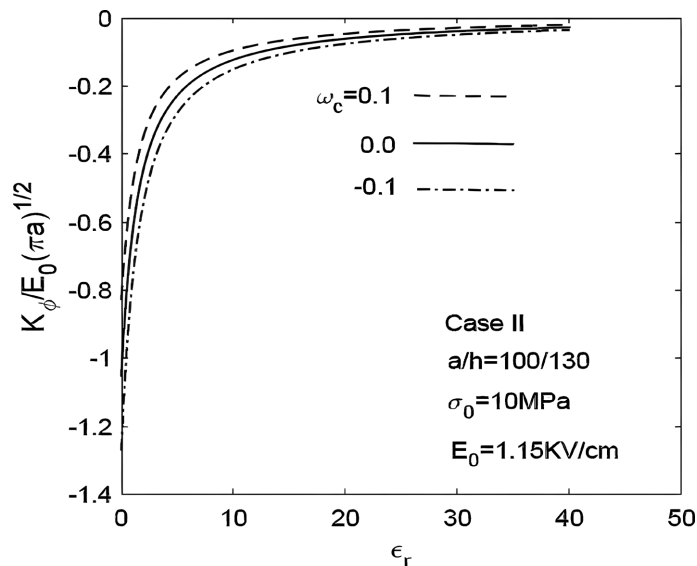


Figure 4. The variations of $K_{\phi}/E_0\sqrt{\pi a}$ versus ϵ_r for $E_0 = 1.15 \text{ KV/cm}$, $\sigma_0 = 10 \text{ MPa}$, $a/h = 100/130$ and $\omega_c = -0.1, 0, 0.1$ under Case I Case II, respectively

图 4. 情形 II 中 $K_{\phi}/E_0\sqrt{\pi a}$ 随 ϵ_r 在 $E_0 = 1.15 \text{ KV/cm}$, $\sigma_0 = 10 \text{ MPa}$, $a/h = 100/130$ 以及 $\omega_c = -0.1, 0, 0.1$ 的变化趋势

5. 结论

本研究中, 在施加有机电荷载作用下, 讨论了一种具有 Griffith 裂纹的压电带型的问题。基于压电材料裂纹条的实验观测, 讨论了两类边界条件下的实验现象。结论表明了自由法向应力边界条件近似模拟实际情况是可行的并且数值结果也表明了该模型的适用性。

参考文献

- [1] Ishihara, M. and Noda, N. (2005) Control of Thermal Stress Intensity Factor in a Piezothermoelastic Semi-Infinite Body with an Edge Crack. *European Journal of Mechanics A/Solids*, **24**, 417-426. <https://doi.org/10.1016/j.euromechsol.2005.01.009>
- [2] Schneider, G.A., Felten, F. and McMeeking, R.M. (2003) The Electrical Potential Difference across Cracks in PZT Measured by Kelvin Probe Microscopy and the Implications for Fracture. *Acta Materialia*, **51**, 2235-2241. [https://doi.org/10.1016/s1359-6454\(03\)00027-2](https://doi.org/10.1016/s1359-6454(03)00027-2)
- [3] Zhang, T.Y., Zhao, M.H. and Gao, C.F. (2005) The Strip Dielectric Breakdown Model. *International Journal of Fracture*, **132**, 311-327. <https://doi.org/10.1007/s10704-005-2054-8>
- [4] Zhu, T. and Yang, W. (1997) Toughness Variation of Ferroelectrics by Polarization Switch under Non-Uniform Electric Field. *Acta Materialia*, **45**, 4695-4702. [https://doi.org/10.1016/s1359-6454\(97\)00123-7](https://doi.org/10.1016/s1359-6454(97)00123-7)
- [5] Ricoeur, A. and Kuna, M. (2009) Electrostatic Traction at Crack Faces and Their Influence on the Fracture Mechanics of Piezoelectrics. *International Journal of Fracture*, **157**, 3-12. <https://doi.org/10.1007/s10704-009-9321-z>
- [6] Zikun, W. (1994) Penny-Shaped Crack in Transversely Isotropic Piezoelectric Materials. *Acta Mechanica Sinica*, **10**, 49-60. <https://doi.org/10.1007/bf02487657>
- [7] Zhong, X.C. (2011) Fracture Analysis of a Piezoelectric Layer with a Penny-Shaped and Energetically Consistent Crack. *Acta Mechanica*, **223**, 331-345. <https://doi.org/10.1007/s00707-011-0565-0>
- [8] Li, X.F. and Lee, K.Y. (2004) Effects of Electric Field on Crack Growth for a Penny-Shaped Dielectric Crack in a Piezoelectric Layer. *Journal of the Mechanics and Physics of Solids*, **52**, 2079-2100. <https://doi.org/10.1016/j.jmps.2004.02.012>
- [9] Guo, J.H., Lu, Z.X., Han, H.T., et al. (2010) The Behavior of Two Non-Symmetrical Permeable Cracks Emanating from an Elliptical Hole in a Piezoelectric Solid. *European Journal of Mechanics A/Solids*, **29**, 654-663. <https://doi.org/10.1016/j.euromechsol.2010.01.001>

-
- [10] Guo, J.H., Lu, Z.X., Han, H.T., *et al.* (2009) Exact Solutions for Anti-Plane Problem of Two Asymmetrical Edge Cracks Emanating from an Elliptical Hole in a Piezoelectric Material. *International Journal of Solids and Structures*, **46**, 3799-3809. <https://doi.org/10.1016/j.ijsolstr.2009.07.002>
- [11] Zhong, X.C. and Zhang, K.S. (2010) Electroelastic Analysis of an Electrically Dielectric Griffith Crack in a Piezoelectric Layer. *International Journal of Engineering Science*, **48**, 612-623. <https://doi.org/10.1016/j.ijengsci.2010.02.002>
- [12] Ueda, S. (2006) The Crack Problem in Piezoelectric Strip under Thermoelastic Loading. *Journal of Thermal Stresses*, **29**, 295-316. <https://doi.org/10.1080/01495730500360450>
- [13] Chen, Z.T. (2006) Dynamic Fracture Mechanics Study of an Electrically Impermeable Mode III Crack in a Transversely Isotropic Piezoelectric Material under Pure Electric Load. *International Journal of Fracture*, **141**, 395-402. <https://doi.org/10.1007/s10704-006-9003-z>
- [14] Nowacki, W. (1978) Some General Theorems of Thermopiezoelectricity. *Journal of Thermal Stresses*, **1**, 171-182. <https://doi.org/10.1080/01495737808926940>

附录 A

$\alpha_j (j=1,2,3)$ 是以下特征方程的根:

$$\begin{vmatrix} c_{11} - c_{44}\alpha^2 & -(c_{13} + c_{44})\alpha & -(e_{31} + e_{15})\alpha \\ -(c_{13} + c_{44})\alpha & c_{33}\alpha^2 - c_{44} & e_{33}\alpha^2 - e_{15} \\ -(e_{31} + e_{15})\alpha & e_{33}\alpha^2 - e_{15} & \varepsilon_{11} - \varepsilon_{33}\alpha^2 \end{vmatrix} = 0.$$

常数 η_{3j} 和 η_{4j} 通过下式求得:

$$\begin{aligned} \alpha_j^2 &= \frac{c_{11}}{c_{44} + (c_{13} + c_{44})\eta_{3j} + (e_{31} + e_{15})\eta_{4j}} \\ &= \frac{c_{13} + c_{44} + c_{44}\eta_{3j} + e_{15}\eta_{4j}}{c_{33}\eta_{3j} + e_{33}\eta_{4j}} \\ &= \frac{e_{31} + e_{15} + e_{15}\eta_{3j} - \varepsilon_{11}\eta_{4j}}{e_{33}\eta_{3j} - \varepsilon_{33}\eta_{4j}}. \end{aligned}$$

常数 $\gamma_{kj} (k=0,1,2,3,4)$ 表示如下:

$$\begin{aligned} \gamma_{0j} &= c_{11} - (c_{33}\eta_{3j} + e_{31}\eta_{4j})\alpha_j^2, \\ \gamma_{1j} &= c_{13} - (c_{33}\eta_{3j} + e_{31}\eta_{4j})\alpha_j^2, \\ \gamma_{2j} &= e_{31} - (e_{33}\eta_{3j} - \varepsilon_{33}\eta_{4j})\alpha_j^2, \\ \gamma_{3j} &= -[c_{44}(1 + \eta_{3j}) + e_{15}\eta_{4j}]\alpha_j, \\ \gamma_{4j} &= -[e_{15}(1 - \eta_{3j}) + \varepsilon_{11}\eta_{4j}]\alpha_j. \end{aligned}$$

函数 $\kappa_{ij}(\bar{s}, \bar{x}) (i, j=1, 2, 3)$ 表达式如下:

$$\begin{aligned} \kappa_{11}(\bar{s}, \bar{x}) &= a \int_0^\infty \sum_{i=1}^3 \gamma_{1i} b_{i1}(\xi) \cos(a\bar{s}\xi) \cos(a\bar{x}\xi) d\xi, \\ \kappa_{12}(\bar{s}, \bar{x}) &= a \int_0^\infty \left[\sum_{i=1}^3 \gamma_{1i} b_{i2}(\xi) - x_{12} \right] \sin(a\bar{s}\xi) \cos(a\bar{x}\xi) d\xi, \\ \kappa_{13}(\bar{s}, \bar{x}) &= a \int_0^\infty \left[\sum_{i=1}^3 \gamma_{1i} b_{i3}(\xi) - x_{13} \right] \sin(a\bar{s}\xi) \cos(a\bar{x}\xi) d\xi, \\ \kappa_{21}(\bar{s}, \bar{x}) &= a \int_0^\infty \sum_{i=1}^3 \gamma_{2i} b_{i1}(\xi) \cos(a\bar{s}\xi) \cos(a\bar{x}\xi) d\xi, \\ \kappa_{22}(\bar{s}, \bar{x}) &= a \int_0^\infty \left[\sum_{i=1}^3 \gamma_{2i} b_{i2}(\xi) - x_{22} \right] \sin(a\bar{s}\xi) \cos(a\bar{x}\xi) d\xi, \\ \kappa_{23}(\bar{s}, \bar{x}) &= a \int_0^\infty \left[\sum_{i=1}^3 \gamma_{2i} b_{i3}(\xi) - x_{23} \right] \sin(a\bar{s}\xi) \cos(a\bar{x}\xi) d\xi, \\ \kappa_{31}(\bar{s}, \bar{x}) &= a \int_0^\infty \left[\sum_{i=1}^3 \gamma_{3i} b_{(i+6)1}(\xi) - x_{31} \right] \cos(a\bar{s}\xi) \sin(a\bar{x}\xi) d\xi, \\ \kappa_{32}(\bar{s}, \bar{x}) &= a \int_0^\infty \sum_{i=1}^3 \gamma_{3i} b_{(i+6)2}(\xi) \sin(a\bar{s}\xi) \sin(a\bar{x}\xi) d\xi, \\ \kappa_{33}(\bar{s}, \bar{x}) &= a \int_0^\infty \sum_{i=1}^3 \gamma_{3i} b_{(i+6)3}(\xi) \sin(a\bar{s}\xi) \sin(a\bar{x}\xi) d\xi. \end{aligned}$$